

EXPERIMENTAL STUDY ON STRENGTH DEVELOPMENT AND ADIABATIC TEMPERATURE OF HIGH-STRENGTH CONCRETE FOR BRIDGE PIERS

Trong Chuc Nguyen^{1,*}, Van Hung Le¹, Quoc Long Hoang¹

¹*Institute of Techniques for Special Engineering, Le Quy Don Technical University*

Abstract

This article presents the design and experimental evaluation of a high-strength concrete mix for bridge pier applications, targeting a compressive strength of 50 MPa. The mix composition was designed according to ACI 211.1-91, incorporating cement, fly ash, blast furnace slag, superplasticizer, and a temperature rise inhibitor. The selected mix achieved a laboratory design strength of 60 MPa. Strength development tests were conducted on cubic and cylindrical specimens at 3, 7, 28, and 56 days. Results showed a compressive strength increase from 35.2 MPa at 3 days to 64.2 MPa at 56 days, while splitting tensile strength improved from 3.12 MPa to 5.19 MPa within the same period. The elastic modulus calculated according to CEB-FIP Model Code 2010, reached 40.47 GPa at 56 days. In addition, an adiabatic calorimeter was designed and improved to monitor the temperature rise of the concrete. Measurements revealed a maximum adiabatic temperature of 76.6°C, corresponding to a temperature rise of 52°C, with the most rapid increase occurring between 8 and 32 hours after casting. The study results provide the necessary data to evaluate the thermal behavior and minimize the risk of thermal cracking in large concrete structures such as bridge piers.

Keywords: *Mass concrete; cement hydration; temperature differential; thermal cracking risk.*

1. Introduction

Mass concrete is increasingly utilized in construction projects, particularly in large-scale structures such as bridge abutments, piers, thick walls, and dams [1]. In transportation infrastructure construction, a substantial volume of concrete, ranging from tens to thousands of cubic meters, is employed. To achieve a structure that not only ensures strength but also provides long-term durability, mass concrete structures must be properly designed, mixed, placed, and cured according to established procedures [2]. The curing period for all mass concrete structures should be continuously maintained for no less than 7 days (under natural conditions), ensuring the attainment of critical curing strength [3]. Furthermore, the construction process must ensure that the structure does not experience cracking due to the thermal effects of cement hydration [4]. Therefore, the

* Corresponding author, email: trongchuc.nguyen@lqdtu.edu.vn
DOI: [10.56651/lqdtu.jst.v8.n2.1074.sce](https://doi.org/10.56651/lqdtu.jst.v8.n2.1074.sce)

incorporation of mineral admixtures, specifically fly ash and ground granulated blast-furnace slag, as a partial replacement for cement in mass concrete structures for transportation infrastructure, is essential.

Partial replacement of cement with fly ash is advantageous as it aids in improving workability, reducing cost, and decreasing the heat of hydration of concrete, which is beneficial for mass concrete structures. However, the early-age strength development rate of concrete typically proceeds slowly [5]-[7]. According to the technical guideline "Using ground granulated blast-furnace slag as a mineral admixture for concrete production," the ability to maintain the workability of concrete mixtures containing blast-furnace slag is superior to that of ordinary Portland cement concrete; although the strength development process is slow at early ages, it achieves or exceeds the strength of ordinary Portland cement concrete after 28 days [8]. Currently, three- or four-component binder material blends are often designed to compensate for deficiencies in the properties of Portland cement or two-component cementitious blends, with the aim of producing concrete with the required mechanical and physical properties for construction projects [9]. Among these, the combination of cement with fly ash and ground granulated blast-furnace slag is commonly employed and shows an increasing trend [10]. In addition to mineral admixtures, temperature rise inhibitor (TRI) is also increasingly utilized in mass concrete structures. TRI functions by retarding the cement hydration heat process, reducing the rate of heat evolution, and thereby helping the structure mitigate the risk of thermal cracking [11].

Temperature rise inhibitor (TRI) is a novel concrete admixture engineered to retard the rate of heat evolution during the acceleration phase of cement hydration without altering the total heat of hydration. Derived from the hydrolysis of corn starch, TRI incorporates hydroxy acid salts and minerals, which are instrumental in mitigating thermal cracking in mass concrete structures. Its operational mechanism involves slow dissolution in alkaline solution, followed by adsorption onto the surface of cement particles and hydration products, thereby inhibiting the reaction rate. Distinct from set-retarding admixtures, TRI does not induce an increase in peak temperature following the gel formation stage; instead, it concurrently reduces both the rate and the maximum temperature value, consequently limiting early-age thermal cracking. Simultaneously, C-S-H formation remains stable, ensuring that the ultimate concrete strength is not compromised. The specific dosage of TRI is product-dependent and subject to manufacturer's recommendations [11]. However, there is a recognized paucity of research investigating the combined influence of fly ash, ground granulated blast-furnace slag (GGBS), and TRI on concrete strength development.

Despite extensive research interest from numerous scientists, several limitations persist. Specifically, the TRI, a modern material additive, has not been thoroughly investigated by Vietnamese researchers. Furthermore, the determination of thermal properties due to cement hydration has primarily relied on the Japanese standard (JCI 2018) for establishing adiabatic temperature curves [12]. This leads to unreliable results when concrete mixes have different composition and curing conditions than Japanese standards.

In this study, the authors conducted experimental research to determine the mechanical and thermal properties of concrete mixes. The research results are important input parameters in the design and prediction of the formation of temperature and stress fields in mass concrete structures. From there, appropriate measures are proposed to prevent thermal cracks in mass concrete structures.

2. Materials and methods

2.1. Materials

2.1.1. Cement

According to TCVN 9035:2011, for mass concrete structures in general construction, the type of cement used is low-heat Portland cement or low-heat blended Portland cement [13]. Furthermore, as per TCVN 7712:2013 [14] and TCVN 6260:2009 [15], low-heat blended Portland cement can be produced by thoroughly mixing finely ground mineral admixtures with Portland cement. Therefore, this study selected PC40 Portland cement for designing the concrete mix composition. The cement used was PC40 But Son Portland cement, with a specific mass of 3.15 g/cm^3 and a specific surface area of $0.364 \text{ m}^2/\text{g}$; its chemical composition is presented in Tab. 1.

2.1.2. Fly ash

The study utilized Pha Lai Class F fly ash, complying with the requirements of TCVN 10302:2014 [16]. The fly ash had a specific mass of 2.35 g/cm^3 , a specific surface area of $0.58 \text{ m}^2/\text{g}$, a dry bulk density in compacted state of 1480 kg/m^3 , and its chemical composition is shown in Tab. 1.

2.1.3. Ground granulated blast furnace slag

Hoa Phat S95 finely ground granulated blast furnace slag (GGBFS) was used in the study. It meets the requirements of TCVN 11586:2016 standard [17]. S95 finely GGBFS has a density of 2.92 g/cm^3 , specific surface area of $0.37 \text{ m}^2/\text{g}$, dry volumetric mass in the compacted state of 1450 kg/m^3 and the chemical composition of granulated blast furnace slag is shown in Tab. 1.

Tab. 1. Chemical composition of cement, fly ash, and ground granulated blast furnace slag, %

	SiO ₂	Al ₂ O ₃	Fe ₂ O ₃	SO ₃	K ₂ O	Na ₂ O	MgO	CaO	P ₂ O ₅	Loss on heating
Cement	20.4	4.4	5.4	3.4	1.2	0.3	2.5	60.2	-	2.2
Fly ash	54.2	23.3	9.8	2.5	1.4	1.1	0.6	1.2	1.4	4.5
GGBFS	36.6	12.6	3.4	5.7	0.4	0.3	-	40.1	-	1.2

2.1.4. Temperature rise inhibitor

The temperature rise inhibitor used in this study is a dextrin organic polymer blend produced by Guangzhou Huakeli Building Materials Co., Ltd. TRI has a variety of cyclodextrin cross-linked macromolecular structures formed in the β -cyclodextrin reaction. Figure 1 shows the Fourier transform infrared spectrum of TRI, which shows that it is mainly composed of dextrin, a polysaccharide (a type of starch) made of glucose molecules, with hydroxyl groups (-OH), methylene groups (-CH-), glycosidic bonds (C-O-C), and carbon-hydrogen bonds (C-H) [11].

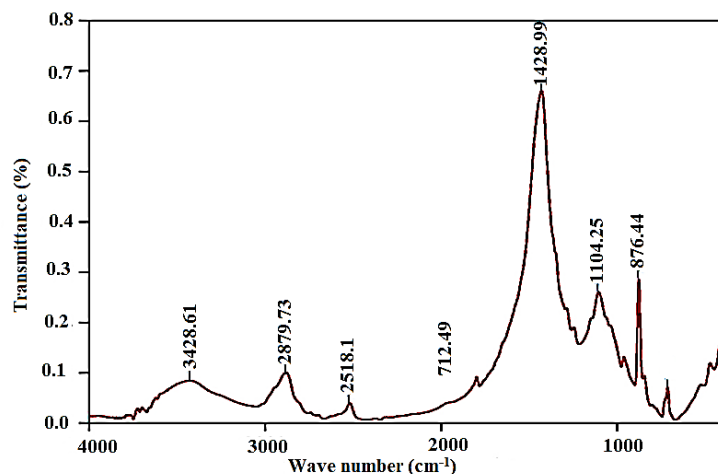


Fig. 1. FTIR spectrum of TRI.

2.1.5. Superplasticizer

The superplasticizer (SP) employed was MasterGlenium SKY 8613. The recommended dosage ranges from 0.5 liters to 2.0 liters per 100 kg of binder, with a typical dosage being 1.0 liters to 1.8 liters per 100 kg of binder.

2.1.6. Coarse aggregate

Crushed stone at Phu Ly quarry, Ha Nam was used for the experiment. The study selected stone with $D_{max} = 20$ mm to design the concrete mix composition. The physical and mechanical parameters are shown in Tab. 2, the grain composition of the stone is shown as the graph in Fig. 2.

Tab. 2. Physical and mechanical properties of coarse aggregate and sand

No.	Parameter	Unit	Standard, TCVN [18]	Coarse aggregate test result	Sand test result
1	Specific mass	g/cm ³	7572:2006	2.72	2.62
2	Dry bulk density	g/cm ³	7572:2006	2.605	2.472
3	Saturated surface dry bulk density	g/cm ³	7572:2006	2.632	2.526
4	Void ratio	g/cm ³	7572:2006	1.482	1.470
5	Dry rodded unit mass	g/cm ³	7572:2006	1.69	1.650
6	Water absorption	%	7572:2006	0.62	1.15

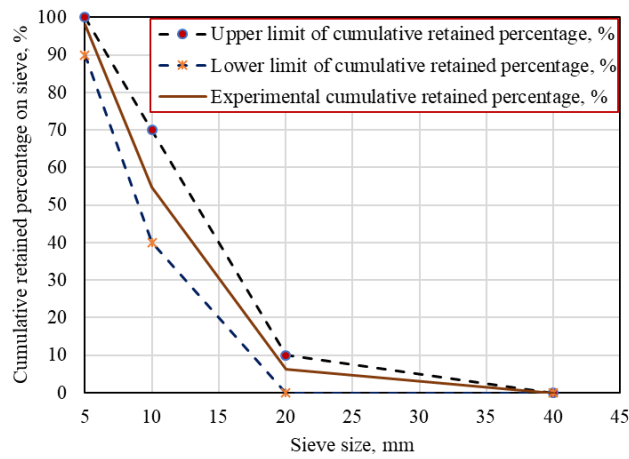


Fig. 2. Particle size distribution chart of coarse aggregate according to TCVN 7570:2006.

2.1.7. Sand

The experiments used coarse yellow sand as fine aggregate. The physical and mechanical properties are presented in Tab. 2, the grain size of the sand is shown as the graph in Fig. 3.

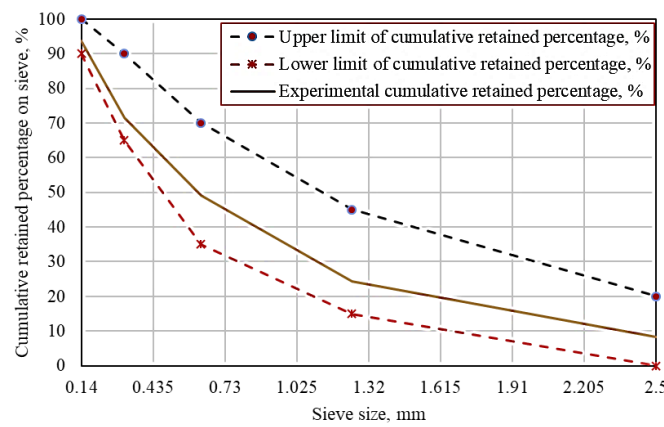


Fig. 3. Sand particle size distribution chart according to TCVN 7570:2006.

2.2. Experimental methods

The compressive strength of concrete was determined according to TCVN 3118:2022 [19].

The concrete used in the study is heavy concrete and the tensile strength is determined by the indirect method. Therefore, the tensile strength is determined by the splitting tensile strength test and is performed according to the standard TCVN 3120:2022 [20].

The experiment to measure the heat of hydration of cement in concrete was performed by the adiabatic method and was conducted according to the Russian standard GOCT 24316-2022 on "Method for determining the heat released during the hardening of concrete" [21].

3. Results and discussion

3.1. Concrete mix design

Because most bridge pier structures meet the requirements of being a reinforced concrete structure, the concrete mix composition is studied and designed according to ACI 211.1-91 standard on "Selection of mix composition for conventional concrete, heavy concrete, and mass concrete" [22].

The concrete mix was designed to achieve a target compressive strength of 50 MPa with a standard sample of $(15 \times 15 \times 15)$ cm. Consequently, the target laboratory design strength was established at 60 MPa.

The results of concrete mix design have obtained many different mixes, depending on the TRI content, fly ash content, and blast furnace slag replacing cement. Therefore, based on ACI 211.1-91 standard, the target concrete strength is 50 MPa, and the reasonable use of fly ash - blast furnace slag - TRI additives according to the ratio of previous studies [22]. In this study, the mix proportion is selected as in Tab. 3 with TRI content accounting for 0.65% of the total binder mass.

Tab. 3. Concrete mix composition

Cement (kg/m ³)	Fly ash (kg/m ³)	Blast furnace slag (kg/m ³)	Sand (kg/m ³)	Coarse aggregate (kg/m ³)	Water (kg/m ³)	Superpl- asticizer (kg/m ³)	TRI (kg/m ³)
322	118	30	757	992	164	4.7	3.06

3.2. Experiment to determine concrete strength

3.2.1. Test to determine compressive strength of concrete (R_n)

The mix was cast into 12 cubes, with standard dimensions of $(15 \times 15 \times 15)$ cm, including 4 groups of samples: Compressive strength at 3 days (R_{n3}), 7 days (R_{n7}),

28 days (R_{n28}) and 56 days (R_{n56}), each group of samples cast 3 samples. The sample compression process is carried out as shown in Fig. 4.



Fig. 4. Experiment to determine the compressive strength of concrete.

For each sample group, the result is taken as the average compressive strength value of 3 sample pieces. The compressive strength results are summarized in Tab. 4. The change in elastic modulus (E) over time was calculated according to the compressive strength test results according to CEB-FIP MODEL CODE 2010 [23], the results are summarized in Tab. 4.

3.2.2. Experiment to determine the tensile strength of concrete when splitting (R_k)

The mix was cast into 12 cylindrical samples with dimensions of $d \times h = 15 \text{ cm} \times 30 \text{ cm}$ (4 sample groups including R_3 , R_7 , R_{28} , R_{56} , and each group cast 3 samples). The split tensile test was performed as shown in Fig. 5.



Fig. 5. Experiment to determine the tensile strength of concrete.

For each set of specimens, the result was taken as the average tensile strength value when splitting of 3 specimens. The tensile strength results when splitting of cylindrical

specimens were converted to standard specimens using a conversion factor of 1.13 [20] and are summarized in Tab. 4.

Tab. 4. Results of strength test and calculation of elastic modulus

Time (day)	R _n , MPa	R _k , MPa	E, GPa
3	35.20	3.12	32
7	47.28	3.82	35.56
28	61.10	4.63	39.31
56	64.23	5.19	40.47

From Tab. 4 we have the following comments: The test results indicate that the compressive strength (R_n), splitting tensile strength (R_k), and elastic modulus (E) of the concrete all increased over time. After 3 days, the compressive strength reached 35.2 MPa (about 70% of the required 50 MPa), showing rapid early-age strength development. At 28 days, the compressive strength reached 61.1 MPa, exceeding the design requirement, and further increased to 64.23 MPa at 56 days. The splitting tensile strength also improved from 3.12 MPa (3 days) to 5.19 MPa (56 days), reflecting consistent growth with compressive strength. The elastic modulus rose steadily from 32 GPa (3 days) to 40.47 GPa (56 days), consistent with the typical development of concrete properties over time. These findings confirm that the designed concrete mix meets strength requirements and ensures long-term performance for bridge structures.

3.3. Experiment to determine adiabatic temperature curve

The study conducted the fabrication of an adiabatic calorimeter according to the model of Y. Lin and H. L. Chen (Fig. 6) [24]. This is the model that Y. Lin and H. L. Chen improved from the adiabatic calorimeter model for concrete materials of G. J. Gibbon [25].

The adiabatic temperature measuring device, which has been custom-fabricated, is illustrated in Fig. 7. Compared with the device of Y. Lin and H. L. Chen, this device has been improved by the author with two additional functions. The first is to add a 3 cm thick layer of foam rubber to prevent evaporation and insulate the surface of the heat preservation chamber. The second is the function of monitoring and collecting results remotely using software that can be installed on mobile phones and computers when connected to the network, without the need for the computer to be directly and continuously connected to the measuring device.

Measure the adiabatic temperature of the concrete sample as follows:

- Prepare and check the measuring equipment, power source, and weigh the material using an electronic scale with an accuracy of 0.1 g. The initial temperature measured in the concrete mixture is 24.6°C.

- Mix the concrete and pour it into the mold containing the sample. Then install the temperature probe at the center of the concrete sample (Fig. 8a).

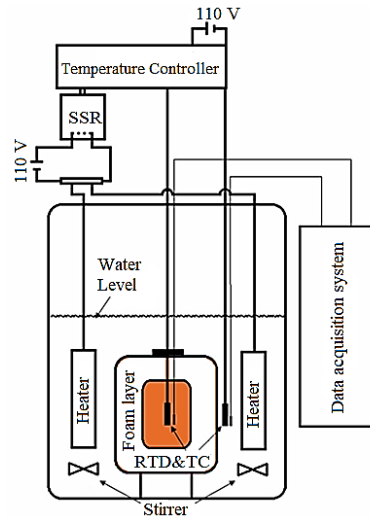


Fig. 6. Adiabatic calorimeter diagram of Y. Lin and H. L. Chen.



Fig. 7. Adiabatic temperature measuring device.



Fig. 8. Preparation for measuring adiabatic temperature of concrete sample.

- Check the initial temperature with the TP300 thermometer (Fig. 8b). Cover the mold and wrap it with plastic to seal between the sample and the water bath. Then, put the mold into the heat chamber, install the temperature sensor on the edge of the mold (Fig. 8c). Install a 3 cm thick rubber sheet on the surface of the heat chamber, then close the lid of the heat chamber (Fig. 8d).

- Install the sensors, power source, network cable, heat chamber with controller and measure the adiabatic temperature (Fig. 9).



Fig. 9. Device for measuring adiabatic temperature.

- Frequency of recording results: Research on setting the frequency of recording measurement results to record once every one minute.

- Adiabatic temperature measurement time: Measurement is carried out until the concrete temperature increases within 24 hours without exceeding 1°C [20].

- Monitor and download measurement results to computer and phone.

- End of measurement: Turn off the power, drain the water, remove the sample mold from the heat-keeping chamber and remove the sample from the mold (Fig. 10).



Fig. 10. Draining and removing sample from container.

The results of adiabatic temperature measurements are shown in Figs. 11, 12. The experiment shows that the temperature develops fastest in the first 48 hours, then the temperature increases gradually and remains almost unchanged at 105 hours.

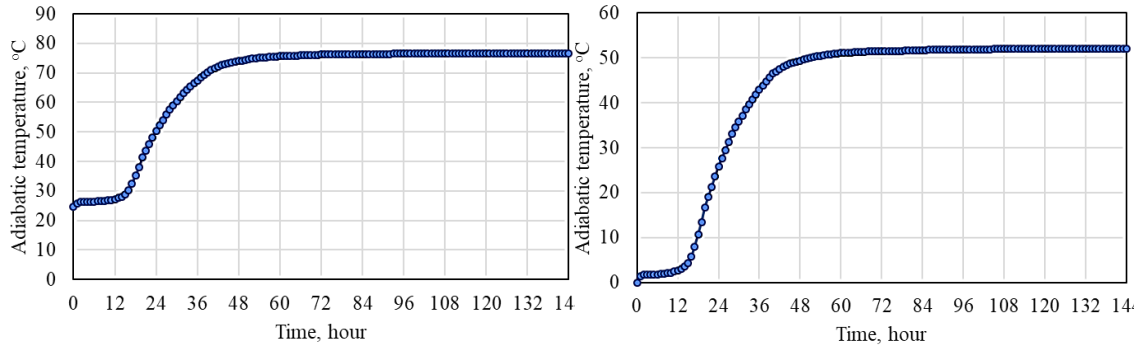


Fig. 11. Adiabatic temperature curve over time.

Fig. 12. Adiabatic temperature increase over time.

Based on the adiabatic curve, we can make the following observations:

- The maximum adiabatic temperature measured is 76.6°C after 105 hours, which means the maximum adiabatic temperature increase is: $\Delta T_{\max} = 76.6 - 24.6 = 52^{\circ}\text{C}$. The adiabatic temperature increase process is shown in the graph in Fig. 13.
- In the first stage from 0 h to 8 h, the temperature increases very slowly, almost stabilizing at $\sim 22\text{--}25^{\circ}\text{C}$. This is the induction period of the cement hydration reaction, the heat release rate is low. This shows that in the first hours after pouring concrete, the heat generation is not significant.
- The rapid increase period from 8 h to 32 h. This is the period of strong temperature increase, from $\sim 25^{\circ}\text{C}$ to $\sim 70^{\circ}\text{C}$. This is the period of strong hydration, high reaction rate, and fast heat release. The fastest rate of increase is around 12-24 hours after pouring. At this stage, it is important to control the temperature, because large temperature differences in the concrete mass can cause thermal stress and thermal cracking.
- Stabilization stage from 32 h to 104 h. The temperature peaks at around $\sim 75\text{--}77^{\circ}\text{C}$ and then stabilizes, remaining almost the same. This is the stage where the hydration reaction gradually decreases, the heat release rate is low.

4. Conclusion

Based on the research results, we draw the following conclusions:

- The study successfully designed a high-strength concrete mix (target 50 MPa, laboratory 60 MPa) using cement, fly ash, slag, superplasticizer, and TRI, suitable for bridge pier applications.

- Experimental results indicated that the mix developed stable mechanical properties over time. The compressive strength increased to 64.2 MPa at 56 days, while the splitting tensile strength reached 5.19 MPa. The elastic modulus also showed a continuous increase, reaching 40.47 GPa, consistent with CEB-FIP Model Code 2010 predictions.

- Adiabatic testing revealed a maximum temperature rise of 52°C, with the critical period between 8-32 hours, underscoring the need for thermal control to prevent cracking in mass concrete.

Acknowledgement

This research is funded by Le Quy Don Technical University Research Fund under the grant number 25.01.55.

References

- [1] Z. Bofang, *Thermal Stresses and Temperature Control of Mass Concrete*. Elsevier, 2014.
- [2] J. Yin, J. Yang, X. Zhang, and L. V. Tao, “Research on application of mass concrete structure in civil building construction”, *The Frontiers of Society, Science and Technology*, Vol. 2, No. 8, pp. 13-16, 2020. DOI: 10.25236/FSST.2020.020803
- [3] *Bê tông - Yêu cầu bảo dưỡng ẩm tự nhiên*, TCVN 8828:2011.
- [4] *Bê tông khối lớn - Thi công và nghiệm thu*, TCVN 9341:2012.
- [5] Z. Li, X. Zhou, H. Ma, and D. Hou, *Advanced Concrete Technology*. John Wiley & Sons, 2022.
- [6] M. D. Niemuth, “Effect of fly ash on the optimum sulfate of Portland cement”, Ph.D. thesis, Purdue University, 2012.
- [7] Viện Vật liệu xây dựng, Bộ Xây dựng. *Chỉ dẫn kỹ thuật “Sử dụng tro bay và cát nghiên, cát biển cho sản xuất bê tông”*, 2021.
- [8] Viện Vật liệu xây dựng, Bộ Xây dựng. *Chỉ dẫn kỹ thuật “Sử dụng xi hạt lò cao nghiên mịn làm phụ gia khoáng cho sản xuất bê tông”*, 2021.
- [9] ACI Committee. *Guide for selecting proportions for high-strength concrete using Portland cement and other cementitious materials*, American Concrete Institute, 2008.
- [10] Reported by ACI Committee 233, ACI 233R-03 “Slag cement in concrete and mortar”.
- [11] Major building materials standards of the People's Republic of China, *JC/T 2608-2021 “Concrete hydration temperature increase inhibitor”*, 2021.
- [12] Japan Concrete Institute, *Guidelines for control of cracking of mass concrete*, 2016.
- [13] *Hướng dẫn lựa chọn xi măng trong xây dựng*, TCVN 9035:2011.
- [14] *Xi măng poóc lăng hỗn hợp ít tỏa nhiệt*, TCVN 7712:2013.
- [15] *Xi măng poóc lăng hỗn hợp - Yêu cầu kỹ thuật*, TCVN 6260:2009.
- [16] *Phụ gia hoạt tính tro bay dùng cho bê tông, vữa xây và xi măng*, TCVN 10302:2014.
- [17] *Xi hạt lò cao nghiên mịn dùng cho bê tông và vữa*, TCVN 11586:2016.

- [18] *Cốt liệu cho bê tông và vữa - Phương pháp thử*, TCVN 7572:2006.
- [19] *Bê tông - Phương pháp xác định cường độ chịu nén*, TCVN 3118:2022.
- [20] *Bê tông - Phương pháp xác định cường độ chịu kéo khi bửa*, TCVN 3120:2022.
- [21] ГОСТ 24316-2022. БЕТОНЫ - Метод определения тепловыделения при твердении.
- [22] American Concrete Institute, *Standard Practice for Selecting Proportions for Normal, Heavyweight, and Mass Concrete. ACI Manual of Concrete Practice*, 1996, pp. 1-38.
- [23] Fédération Internationale du Béton, *Model Code 2010 - Final Draft: Volume 1*, 2012.
- [24] Y. Lin and H. L. Chen, "Thermal analysis and adiabatic calorimetry for early-age concrete members", *Journal of Thermal Analysis and Calorimetry*, Vol. 122, No. 2, pp. 937-945, 2015.
- [25] G. J. Gibbon and Y. Ballim, "Laboratory test procedures to predict the thermal behaviour of concrete", *Journal of the South African Institution of Civil Engineers*, Vol. 38, No. 3, pp. 21-28, 1996.

NGHIÊN CỨU THỰC NGHIỆM VỀ SỰ PHÁT TRIỂN CƯỜNG ĐỘ VÀ NHIỆT ĐỘ ĐOẠN NHIỆT CỦA BÊ TÔNG CƯỜNG ĐỘ CAO CHO TRỤ CẦU

Nguyễn Trọng Chức¹, Lê Văn Hưng¹, Hoàng Quốc Long¹

¹Viện Kỹ thuật công trình đặc biệt, Trường Đại học Kỹ thuật Lê Quý Đôn

Tóm tắt: Bài báo trình bày việc thiết kế và đánh giá thí nghiệm hỗn hợp bê tông cường độ cao sử dụng cho công trình trụ cầu, với cường độ nén 50 MPa. Thành phần hỗn hợp được thiết kế theo ACI 211.1-91, kết hợp xi măng, tro bay, xỉ lò cao, chất siêu dẻo và chất úc ché tăng nhiệt độ. Hỗn hợp được lựa chọn đạt cường độ thiết kế trong phòng thí nghiệm là 60 MPa. Các thí nghiệm xác định cường độ bê tông được tiến hành trên các mẫu hình lập phương và hình trụ ở 3, 7, 28 và 56 ngày. Kết quả cho thấy cường độ nén tăng từ 35,2 MPa sau 3 ngày lên 64,2 MPa sau 56 ngày, trong khi cường độ kéo tách tăng từ 3,12 MPa lên 5,19 MPa trong cùng thời kỳ. Mô đun đàn hồi được tính toán theo Tiêu chuẩn CEB-FIP 2010 đạt 40,47 GPa sau 56 ngày. Ngoài ra, một thiết bị đo đoạn nhiệt đã được thiết kế và cải tiến để theo dõi sự gia tăng nhiệt độ của bê tông. Các phép đo cho thấy nhiệt độ đoạn nhiệt tối đa là 76,6°C, tương ứng với mức tăng đoạn nhiệt là 52°C, với mức tăng nhanh nhất xảy ra trong khoảng từ 8 đến 32 giờ sau khi đổ. Kết quả nghiên cứu cung cấp dữ liệu cần thiết để đánh giá ứng xử nhiệt và giảm thiểu nguy cơ nứt nhiệt trong các kết cấu bê tông khối lớn như trụ cầu.

Từ khóa: Bê tông khối lớn; thủy hóa xi măng; chênh lệch nhiệt độ; nguy cơ nứt nhiệt.

Received: 03/10/2025; Revised: 23/12/2025; Accepted for publication: 26/12/2025

